# Paleohydrologic evolution of the Kambalda gold camp

Klaus Petersen[1], Steffen Hagemann, Peter Neumayr

*Centre for Global Metallogeny, School of Earth & Geographical Sciences, The University of Western Australia, 35 Stirling Highway, Crawley WA 6907, Australia.*

[1] Corresponding author: E-mail, kjpeters@segs.uwa.edu.au

**ABSTRACT**

At the Kambalda gold camp, at least three stages of hydrothermal alteration are distinguished: Stage 1: pre-gold stage with epidote-calcite-magnetite-chalcopyrite alteration, stage 2:syn-gold stage with gold-related plagioclase-dolomite/ankerite-pyrite-hematite±magnetite±pyrrhotite alteration, and stage 3: post-gold stage quartz-carbonate veins. All three alteration stages are characterized by specific hydrothermal fluids.

Stage 1 alteration contains only aqueous fluids with a low salinity (<7.4 wt% NaCl equiv.) and high homogenization temperatures (>250º C) indicating the influx of hot fluids. The origin of the fluid is at present equivocal, but given that the epidote, in equilibrium with magnetite and chalcopyrite, is typically spatially related to porphyry stocks a magmatic-hydrothermal origin of the fluid is likely.

Stage 2 alteration contains chemically complex fluids. Detailed petrographic observations on growth zones in gold-related dolomite indicate that the early stage fluids are aqueous with high salinity (< 23 wt% NaCl equiv.). Main stage hydrothermal fluid changed rapidly to a low salinity $H_2O$-$CO_2$ and $CO_2$-$H_2O$ fluid indicating the influx of a new, high-temperature (> 280ºC) fluid and/or dilution of the original high-salinity aqueous fluid. Importantly, the change in fluid composition is characterized by sudden increase in fluid inclusion size and a rapid decrease in the Fe content and increase in Mn content of the hosting dolomite/ankerite mineral. Together this is taken as evidence of rapid mineral growth, whereas outer zones of the dolomite indicate slow growth. The rapid change in this case is also accompanied by precipitation of scheelite. Laser ICP-MS data indicate that the fluid contained Na, K, Zn, As, V, Rb and Pb at elevated levels. Importantly, fluid densities of the earlier aqueous and the later aqueous-carbonic inclusions can only be interpreted with either a pressure drop or a combined pressure drop and temperature increase during this stage. At present, it is interpreted that the timing of the rapid fluid change and rapid dolomite growth coincides with the onset of pyrite and gold deposition.

Stage 3 alteration contains low-temperature $H_2O \pm CO_2$ fluids; locally fluid inclusions contain daughter minerals (e.g., halite, carbonate) indicating, in combination with dissolution temperatures, high salinities of up to 37 wt% NaCl equiv.

In summary, fluid inclusions at the Kambalda gold camp occur in a range of settings and host minerals (especially in the Revenge and Conqueror gold deposits at St. Ives) and mimic the different hydrothermal alteration stages and host minerals of different relative timing as well as in different fluid pathways of similar timing. Gold deposition appears to coincide with the rapid change in fluid composition from early high salinity aqueous fluid to a low salinity aqueous-carbonic to carbonic fluid. The exact mechanism of how this change was achieved (e.g., fluid mixing and/or phase immiscibility) is currently under investigation.

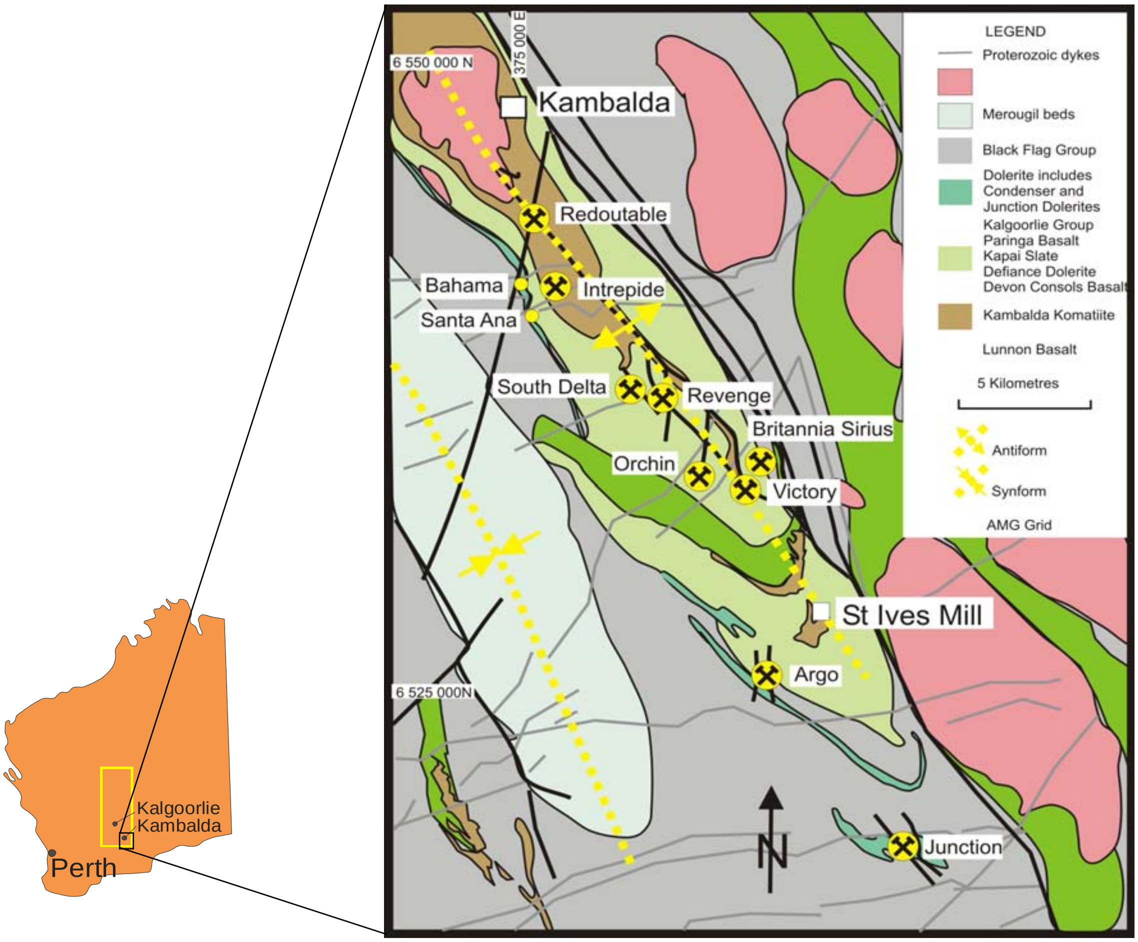


**Fig. 1.** Geological map of the St. Ives gold camp including the location of the major gold deposits.

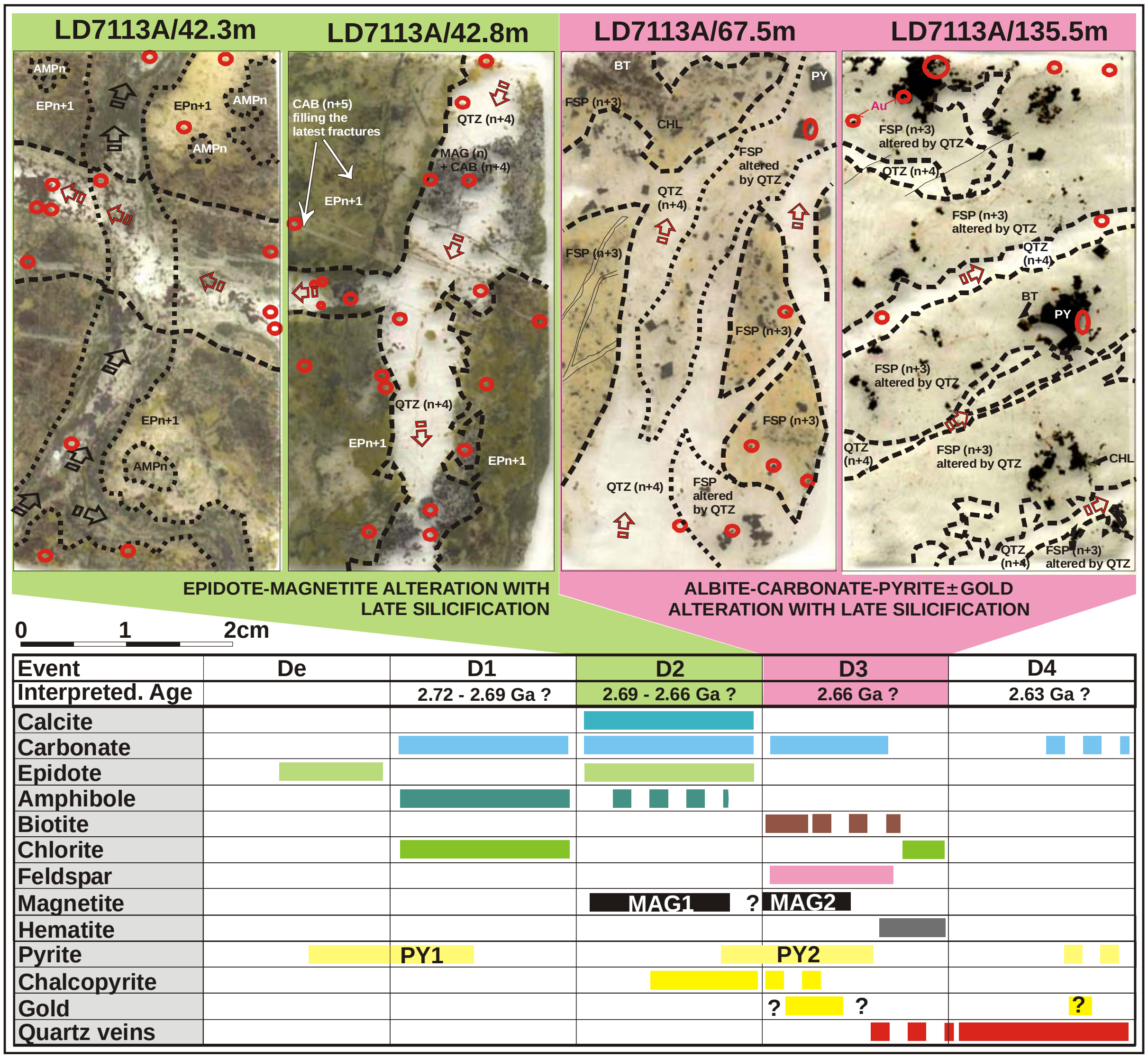


**Fig. 2.** Structural-magmatic-metamorphic-hydrothermal alteration and mineralization chronology.

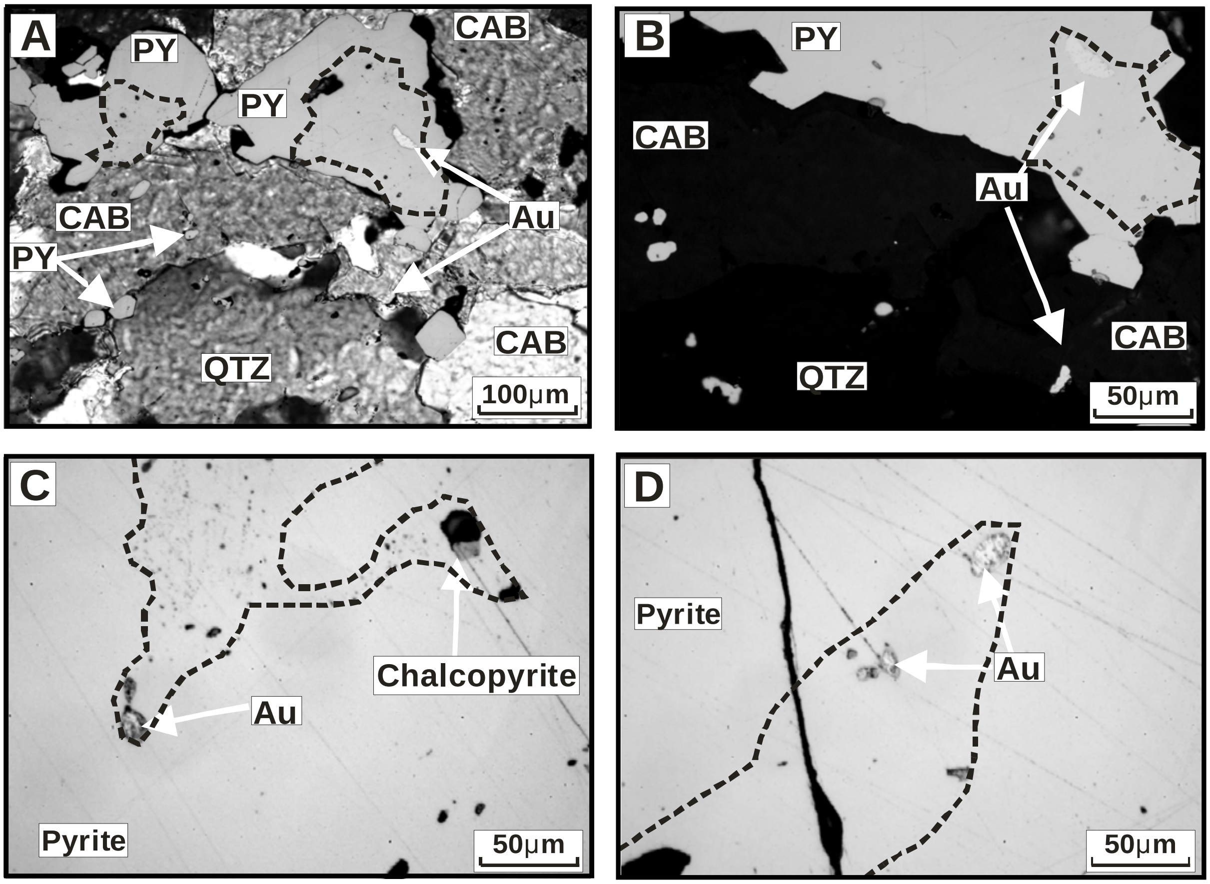


**Fig. 3A.** Photomicrography showing pyrite crystals (stage 2) in the quartz-carbonate vein (stage 3). The pyrite crystals show a zonation (dotted line) of a nucleous with large mineral inclusions (e.g. gold) and a border with smaller mineral inclusions. Gold is related to the "dirty" zonation of pyrite. A small gold grain is displayed in the carbonate probably as a result of the pyrite dissolution and liberation of the gold grain. The quartz-carbonate of stage 3 postdates pyrite because pyrite grains show rounded borders (dissolution) (70% transmitted and 30% reflected light, CD10095W2/372.20m).

**B.** Enlarged image of (A) with reflected light only showing gold grains (CD10095W2/372.20m).

**C.** Pyrite grain with zonation (dotted line) of earlier "dirty" nucleous showing several inclusions together with gold and chalcopyrite (reflected light, LD7113A/135.50m).

**D.** Pyrite grain with gold at the margins of the "dirty" zone and the clean border (reflected light, LD7113A/135.50m).

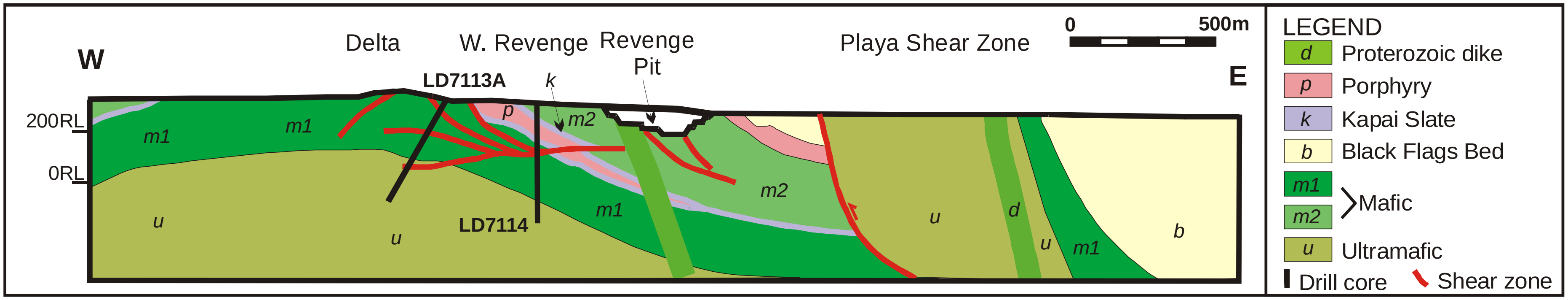


**Fig. 4.** Geological profile at Revenge.

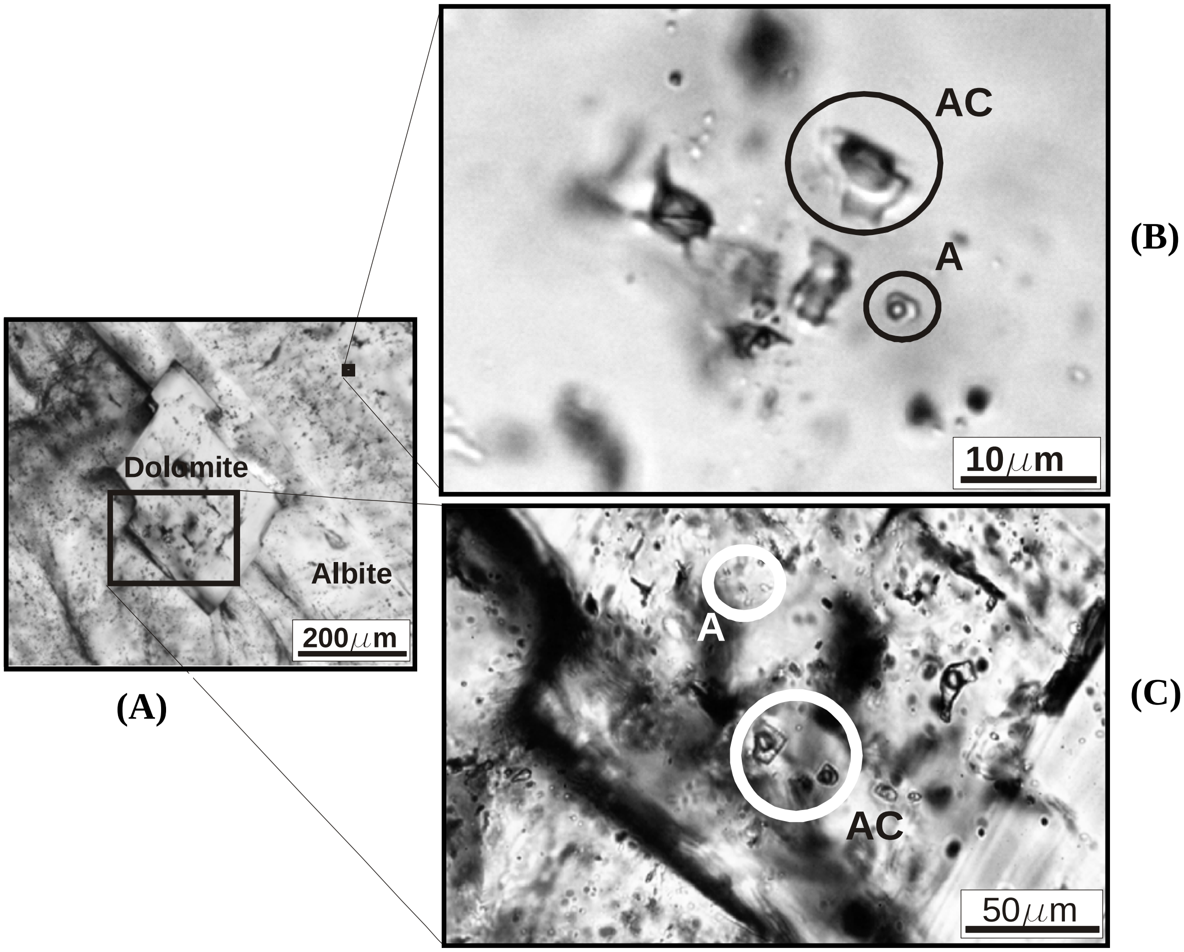


**Fig. 5A.** Group 1 alteration showing a dolomite crystal with crystal growth zonation hosted in albite; **B.** albite showing two generations of fluid inclusion: small earlier aqueous and larger later aqueous-carbonic; **C.** dolomite crystal showing fluid evolution with small aqueous fluid inclusions in the nucleus, large aqueous-carbonic inclusions in the intermediate zone, and medium sized aqueous-carbonic fluid inclusion in the relative clear border.

**Table 1 -** Types and Characteristics of Fluid Inclusions from Stage 1 (epidote-magnetite-calcite), Stage 2 (plagioclase-dolomite/ankerite-pyrite-magnetite-gold), and Stage 3 (quartz-carbonate) from the hydrothermal alteration Revenge gold deposit at the St. Ives Gold Camp. (Timing: P-primary, PS-pseudosecundary; n = number of measurements).

| Stage | Host mineral | Sample location | Fluid inclusion type | Timing | Abundance | Setting | Shape | Size Min to max Average | n | Daughter crystal |
|---|---|---|---|---|---|---|---|---|---|---|
| 1 | Epidote | LD7113A 42.80m | $H_2O$-NaCl | P | Rare | Cluster | Irregular/ Negative crystal | 4 to 20 µm 8.2 µm | 24 | |
| | Quartz | LD7113A 42.80m | $H_2O$-NaCl | P | Rare | Cluster | Regular/ Negative crystal | 4 to 12 µm 8.1 µm | 7 | |
| 2 | Plagioclase | LD7113A 135.50m | $CO_2$ | P | Rare | Cluster | Irregular | 3-10 µm 5.6 µm | 10 | |
| | Albite | LD7113A 135.50m | $CO_2$- $H_2O$-NaCl | P | Rare | Cluster | Irregular | 4 to 7 µm 6.0 µm | 3 | |
| | Albite | LD7114 173.05m | $CO_2$ | P | Rare | Cluster | Irregular/ Regular | 2-9 µm 4.1 µm | 15 | |
| | Albite | LD7114 173.05m | $CO_2$- $H_2O$-NaCl | P | Rare | Cluster | Irregular/ Negative crystal | 11 to 15 µm 13.0 µm | 2 | Rare not determined |
| | Dolomite/ Ankerite | LD7113A 135.50m | $CO_2$- $H_2O$-NaCl | P | Rare | Cluster | Irregular/ Negative crystal | 6-12 µm 7.8 µm | 7 | |
| | Dolomite/ Ankerite | LD7113A 329.30m | $H_2O$-NaCl | P | Rare | Growth zone | Irregular | 4 to 30 µm 8.6 µm | 9 | |
| | Dolomite/ Ankerite | LD7113A 329.30m | $CO_2$- $H_2O$-NaCl | P | Rare | Growth zone | Irregular/ Negative crystal | 5 to 9 µm 5.7 µm | 5 | |
| | Quartz | LD7113A 173.05m | $CO_2$- $H_2O$-NaCl | P | Common | Cluster | Regular | 8 to 20 µm 11.2 µm | 13 | |
| | Quartz | LD7114 67.50m | $CO_2$- $H_2O$-NaCl | P | Common | Cluster | Irregular | 10 to 30 µm 17.2 µm | 21 | Carbonate, halite |
| 3 | Dolomite/ Ankerite | LD7113A 42.80m | $H_2O$-NaCl | P | Common | Trial | Regular | 2 to 15 µm 6.7 µm | 12 | |
| | Dolomite/ Ankerite | LD7113A 135.50m | $H_2O$-NaCl | P | Common | Cluster | Negative crystal | 8 µm 8 µm | 1 | |
| | Dolomite/ Ankerite | LD7114 173.05m | $H_2O$-NaCl | P | Common | Cluster | Irregular | 5 to 6 µm 5.5 µm | 4 | |
| | Dolomite/ Ankerite | LD7114 173.05m | $CO_2$ | P | Common | Cluster | Irregular/ Negative crystal | 3 to 10 µm 5.1 µm | 8 | |
| | Dolomite/ Ankerite | LD7113A 135.50m | $CO_2$- $H_2O$-NaCl | P | Common | Cluster | Regular/ Negative crystal | 3 to 7 µm 4.3 µm | 6 | |
| | Dolomite/ Ankerite | LD7114 173.05m | $CO_2$- $H_2O$-NaCl | P | Common | Cluster | Negative crystal | 4 to 10 µm 5.9 µm | 8 | |
| | Quartz | LD7113A 42.80m | $H_2O$-NaCl | P | Common | Cluster | Irregular | 7 to 15 µm 10.5 µm | 10 | |
| | Quartz | LD7113A 67.50m | $H_2O$-NaCl | P | Common | Cluster | Irregular/ regular | 3 to 15 µm 6.3 µm | 8 | Carbonate, halite |
| | Quartz | LD7113A 135.50m | $H_2O$-NaCl | P/PS | Common | Cluster | Irregular/ regular | 2 to 35 µm 8.05 µm | 44 | Carbonate, halite |
| | Quartz | LD7114 173.05m | $H_2O$-NaCl | P/PS | Common | Trail | Regular/ Negative crystal | 3 to 10 µm 6.7 µm | 10 | Carbonate, halite |
| | Quartz | LD7113A 135.50m | $CO_2$ | P/PS | Common | Cluster | Regular/ Negative crystal | 3 to 25 µm 8.4 µm | 16 | |
| | Quartz | LD7113A 67.50m | $CO_2$- $H_2O$-NaCl | P | Common | Cluster | Negative crystal | 5 µm 5 µm | 1 | |
| | Quartz | LD7113A 135.50m | $CO_2$- $H_2O$-NaCl | P/PS | Common | Cluster | Regular/ Negative crystal | 6 to 30 µm 11.9 µm | 16 | |
| | Quartz | LD7114 173.05m | $CO_2$- $H_2O$-NaCl | P | Common | Cluster | Irregular | 5 to 8 µm 6.5 µm | 6 | Carbonate, halite |

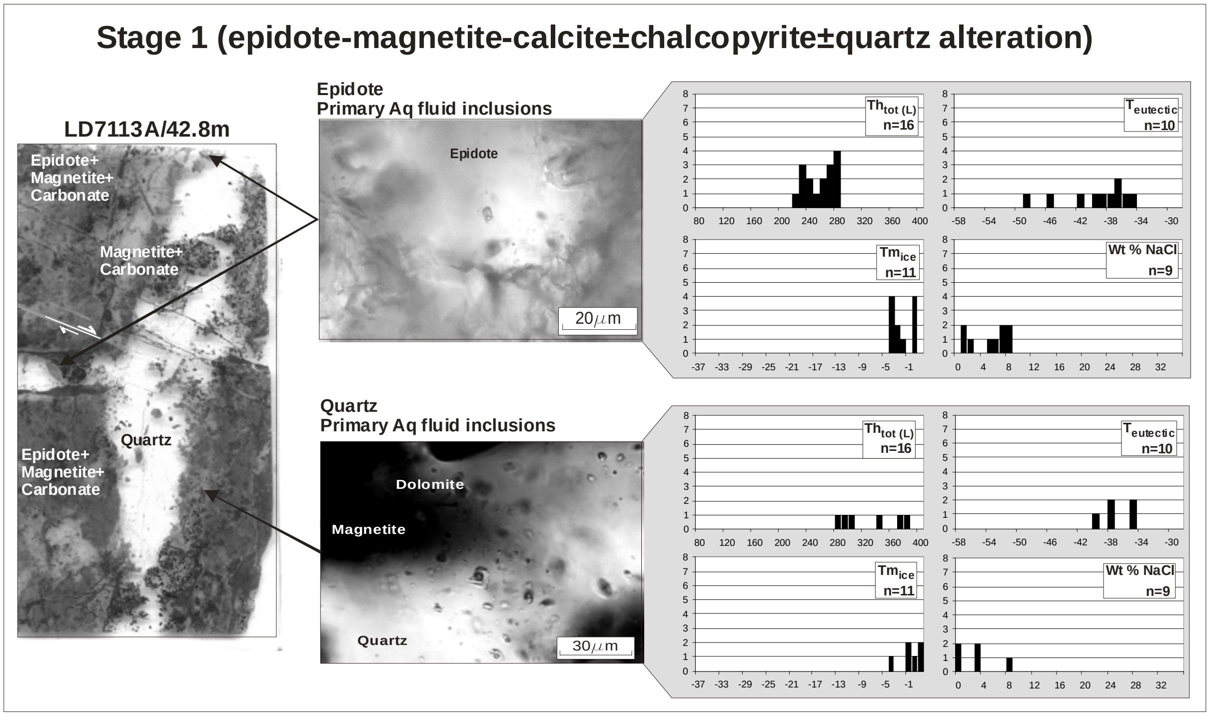


**Fig. 6.** Location and histogram of fluid inclusion data for Stage 1 hydrothermal alteration.

**Table 1 -** Types and Characteristics of Fluid Inclusions from Stage 1 (epidote-magnetite-calcite), Stage 2 (plagioclase-dolomite/ankerite-pyrite-magnetite-gold), and Stage 3 (quartz-carbonate) from the hydrothermal alteration Revenge gold deposit at the St. Ives Gold Camp. (Timing: P-primary, PS-pseudosecundary; n = number of measurements).

| Stage | Host mineral | Sample location | Fluid inclusion type | Timing | Abundance | Setting | Shape | Size Min to max Average | n | Daughter crystal |
|---|---|---|---|---|---|---|---|---|---|---|
| 1 | Epidote | LD7113A 42.80m | $H_2O$-NaCl | P | Rare | Cluster | Irregular/ Negative crystal | 4 to 20 µm 8.2 µm | 24 | |
| | Quartz | LD7113A 42.80m | $H_2O$-NaCl | P | Rare | Cluster | Regular/ Negative crystal | 4 to 12 µm 8.1 µm | 7 | |
| 2 | Plagioclase | LD7113A 135.50m | $CO_2$ | P | Rare | Cluster | Irregular | 3-10 µm 5.6 µm | 10 | |
| | Albite | LD7113A 135.50m | $CO_2$- $H_2O$-NaCl | P | Rare | Cluster | Irregular | 4 to 7 µm 6.0 µm | 3 | |
| | Albite | LD7114 173.05m | $CO_2$ | P | Rare | Cluster | Irregular/ Regular | 2-9 µm 4.1 µm | 15 | |
| | Albite | LD7114 173.05m | $CO_2$- $H_2O$-NaCl | P | Rare | Cluster | Irregular/ Negative crystal | 11 to 15 µm 13.0 µm | 2 | Rare not determined |
| | Dolomite/ Ankerite | LD7113A 135.50m | $CO_2$- $H_2O$-NaCl | P | Rare | Cluster | Irregular/ Negative crystal | 6-12 µm 7.8 µm | 7 | |
| | Dolomite/ Ankerite | LD7113A 329.30m | $H_2O$-NaCl | P | Rare | Growth zone | Irregular | 4 to 30 µm 8.6 µm | 9 | |
| | Dolomite/ Ankerite | LD7113A 329.30m | $CO_2$- $H_2O$-NaCl | P | Rare | Growth zone | Irregular/ Negative crystal | 5 to 9 µm 5.7 µm | 5 | |
| | Quartz | LD7113A 173.05m | $CO_2$- $H_2O$-NaCl | P | Common | Cluster | Regular | 8 to 20 µm 11.2 µm | 13 | |
| | Quartz | LD7114 67.50m | $CO_2$- $H_2O$-NaCl | P | Common | Cluster | Irregular | 10 to 30 µm 17.2 µm | 21 | Carbonate, halite |
| 3 | Dolomite/ Ankerite | LD7113A 42.80m | $H_2O$-NaCl | P | Common | Trial | Regular | 2 to 15 µm 6.7 µm | 12 | |
| | Dolomite/ Ankerite | LD7113A 135.50m | $H_2O$-NaCl | P | Common | Cluster | Negative crystal | 8 µm 8 µm | 1 | |
| | Dolomite/ Ankerite | LD7114 173.05m | $H_2O$-NaCl | P | Common | Cluster | Irregular | 5 to 6 µm 5.5 µm | 4 | |
| | Dolomite/ Ankerite | LD7114 173.05m | $CO_2$ | P | Common | Cluster | Irregular/ Negative crystal | 3 to 10 µm 5.1 µm | 8 | |
| | Dolomite/ Ankerite | LD7113A 135.50m | $CO_2$- $H_2O$-NaCl | P | Common | Cluster | Regular/ Negative crystal | 3 to 7 µm 4.3 µm | 6 | |
| | Dolomite/ Ankerite | LD7114 173.05m | $CO_2$- $H_2O$-NaCl | P | Common | Cluster | Negative crystal | 4 to 10 µm 5.9 µm | 8 | |
| | Quartz | LD7113A 42.80m | $H_2O$-NaCl | P | Common | Cluster | Irregular | 7 to 15 µm 10.5 µm | 10 | |
| | Quartz | LD7113A 67.50m | $H_2O$-NaCl | P | Common | Cluster | Irregular/ regular | 3 to 15 µm 6.3 µm | 8 | Carbonate, halite |
| | Quartz | LD7113A 135.50m | $H_2O$-NaCl | P/PS | Common | Cluster | Irregular/ regular | 2 to 35 µm 8.05 µm | 44 | Carbonate, halite |
| | Quartz | LD7114 173.05m | $H_2O$-NaCl | P/PS | Common | Trail | Regular/ Negative crystal | 3 to 10 µm 6.7 µm | 10 | Carbonate, halite |
| | Quartz | LD7113A 135.50m | $CO_2$ | P/PS | Common | Cluster | Regular/ Negative crystal | 3 to 25 µm 8.4 µm | 16 | |
| | Quartz | LD7113A 67.50m | $CO_2$- $H_2O$-NaCl | P | Common | Cluster | Negative crystal | 5 µm 5 µm | 1 | |
| | Quartz | LD7113A 135.50m | $CO_2$- $H_2O$-NaCl | P/PS | Common | Cluster | Regular/ Negative crystal | 6 to 30 µm 11.9 µm | 16 | |
| | Quartz | LD7114 173.05m | $CO_2$- $H_2O$-NaCl | P | Common | Cluster | Irregular | 5 to 8 µm 6.5 µm | 6 | Carbonate, halite |

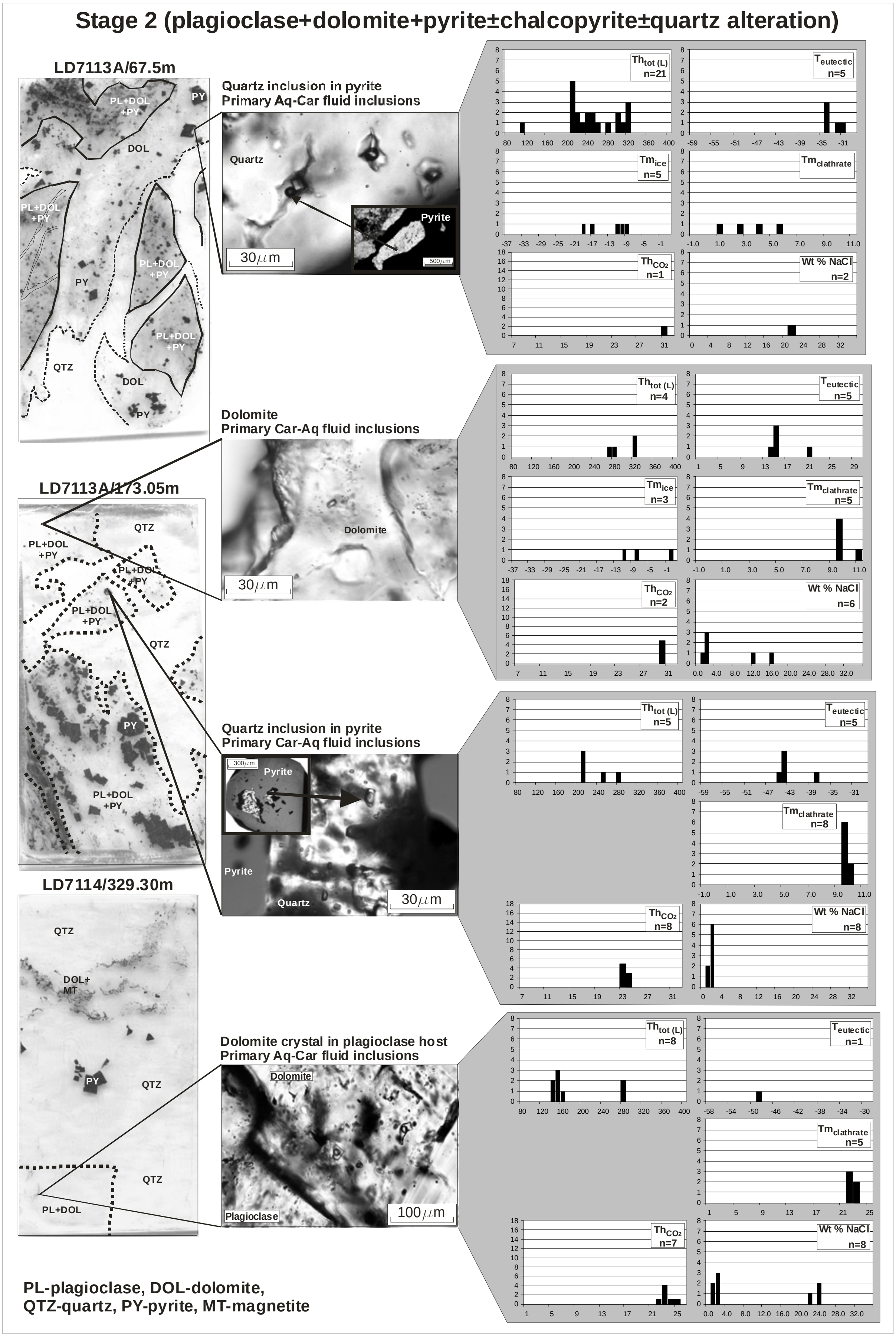


**Fig. 8.** Location and histogram of fluid inclusion data for stage 2 hydrothermal alteration.

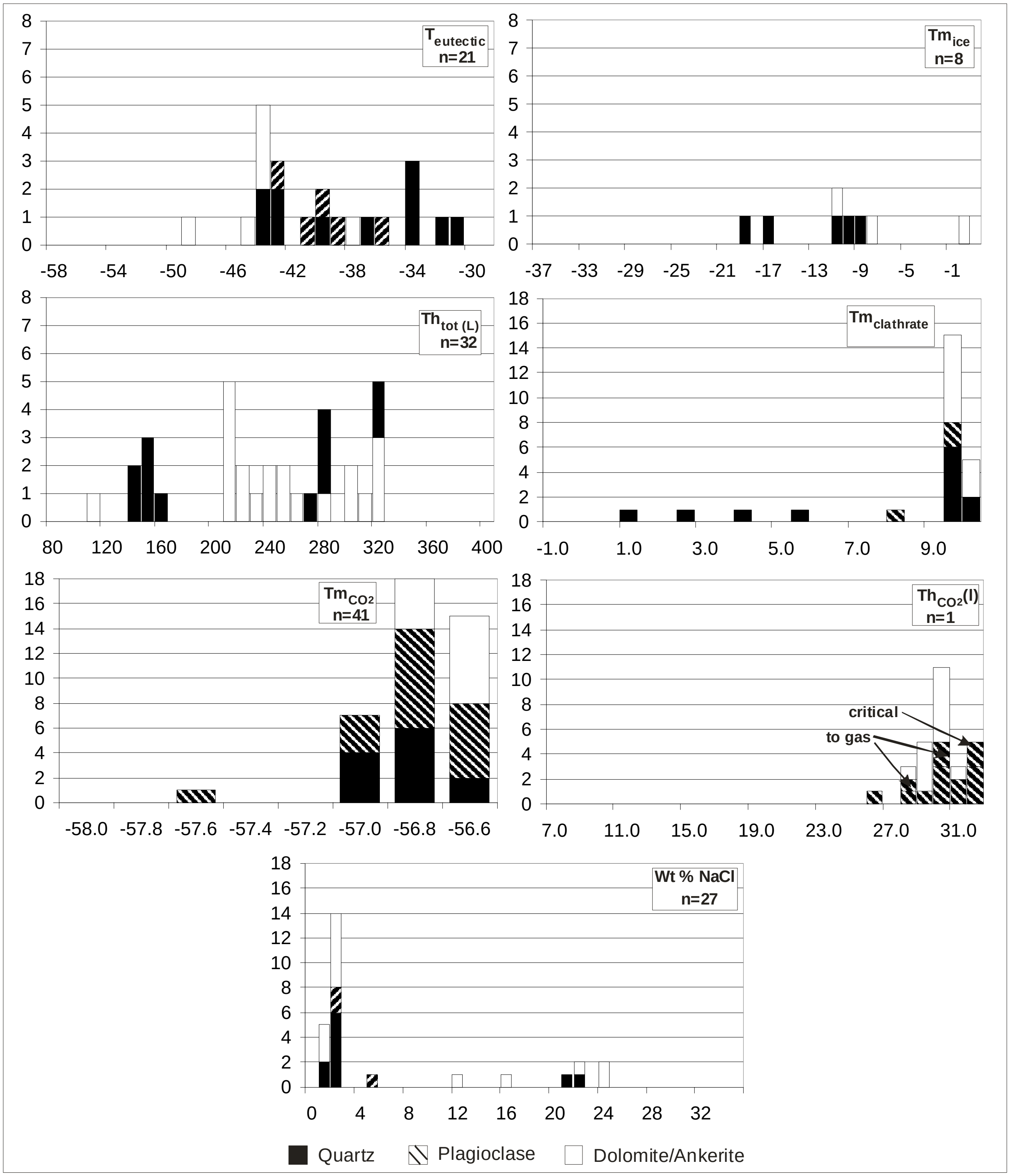


**Fig. 9.** Histogram of all fluid inclusion data for stage 2 hydrothermal alteration.

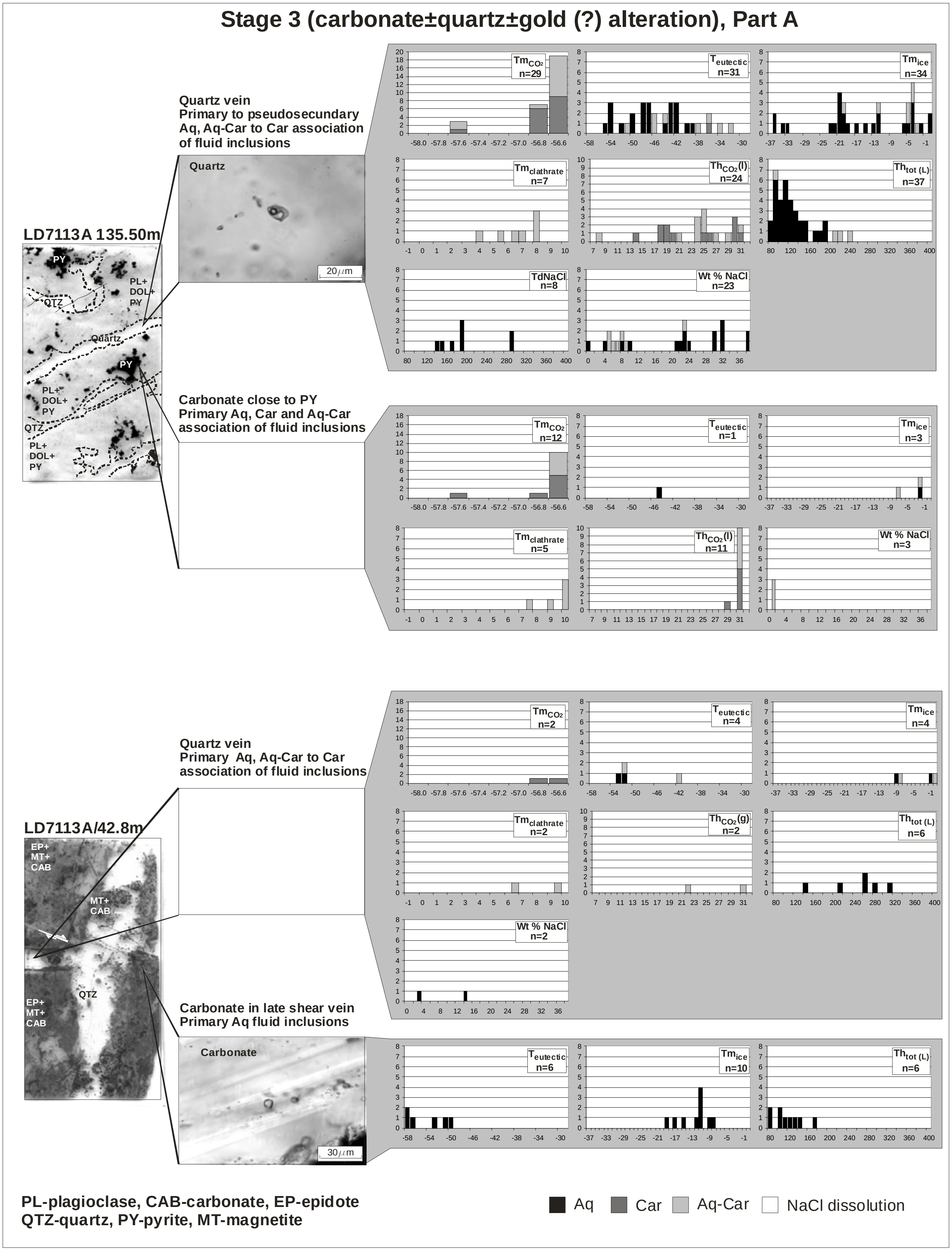


**Fig. 10A.** Location and histogram of fluid inclusion data for stage 3 hydrothermal alteration.

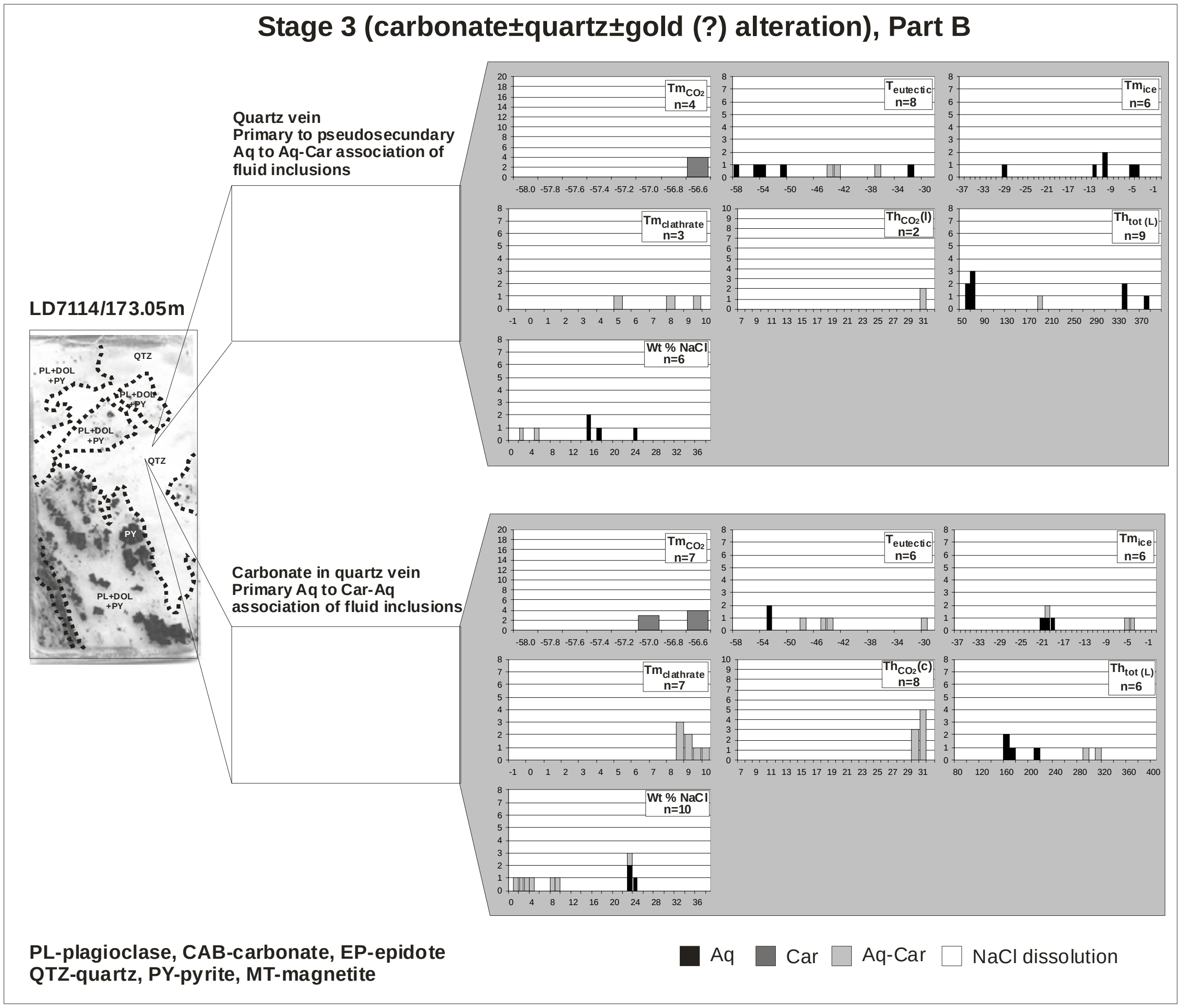


**Fig. 10B.** Location and histogram of fluid inclusion data for stage 3 hydrothermal alteration.

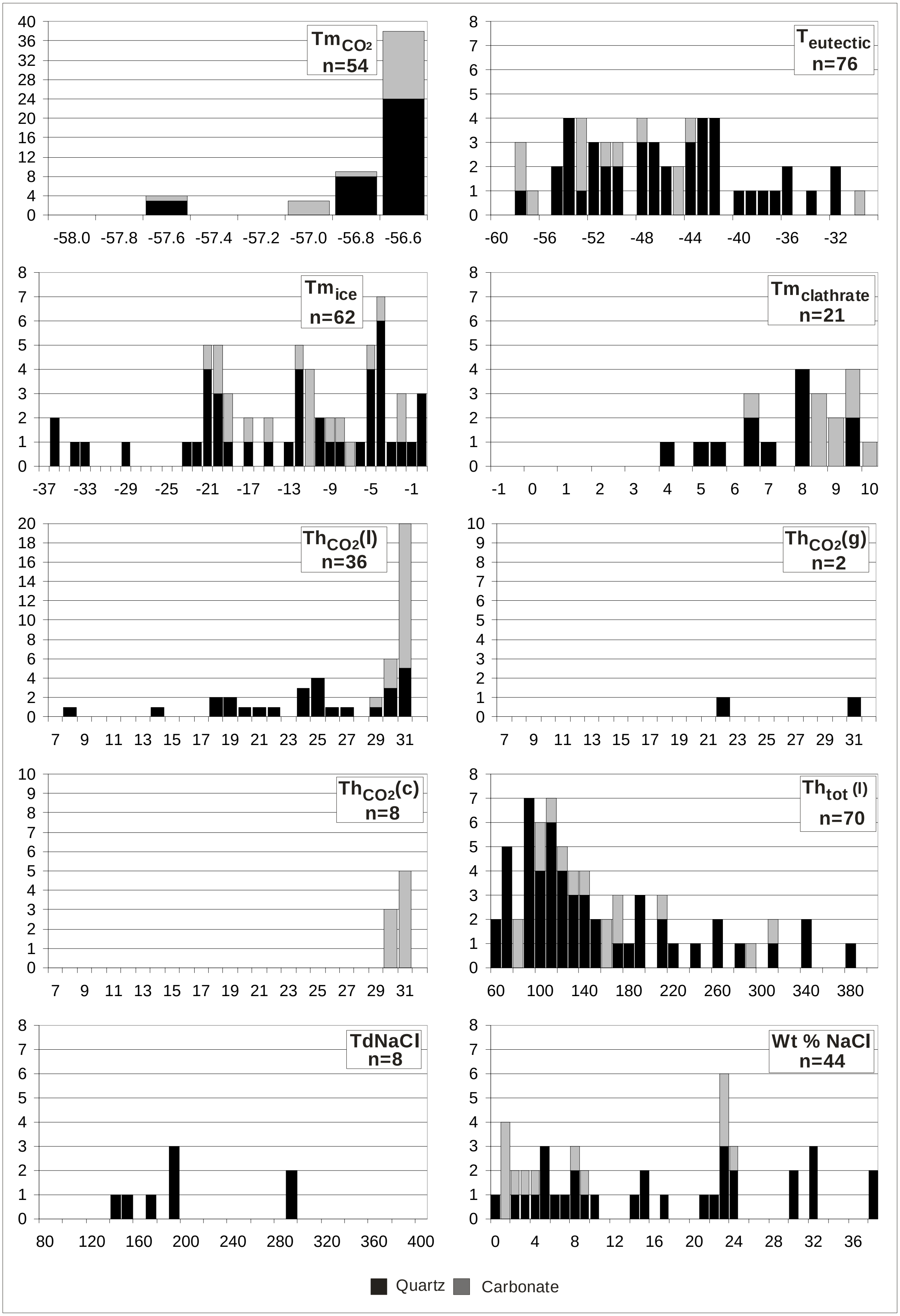


**Fig. 11.** Histogram of all fluid inclusion data for stage 1 hydrothermal alteration.

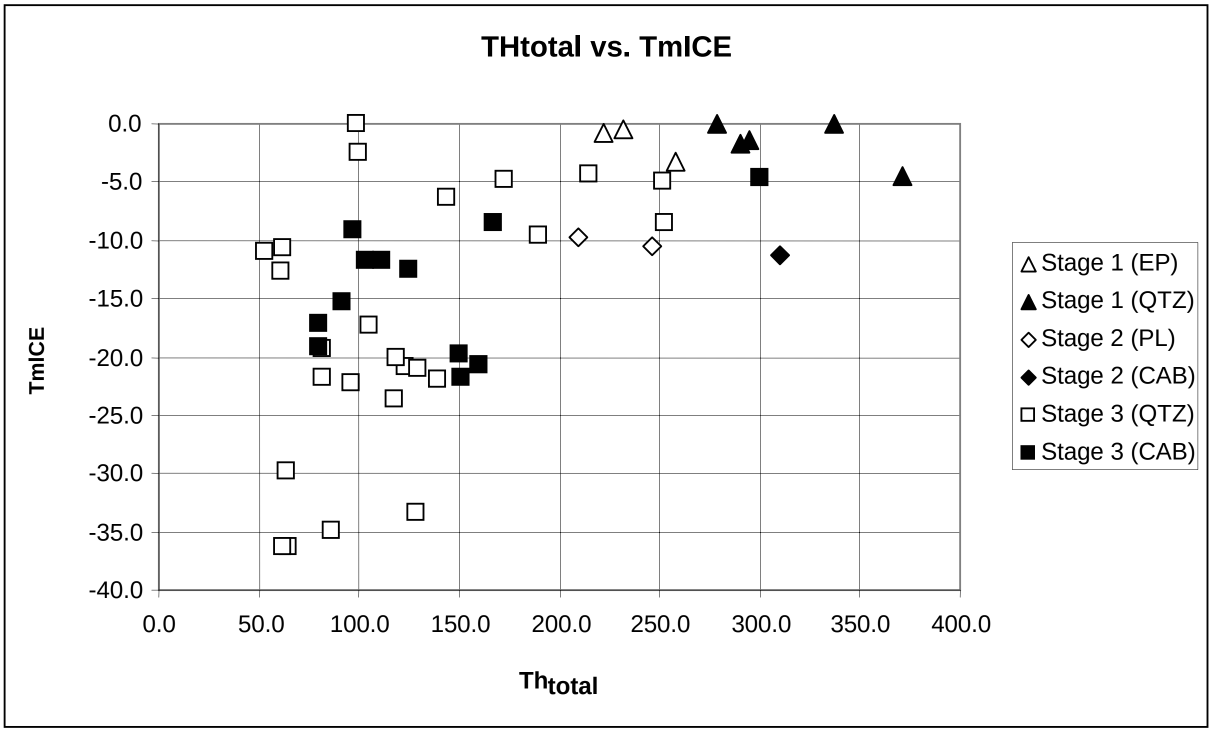


**Fig. 12A.** ThTOT versus TmICE for fluid inclusions from stages 1, 2 and 3.

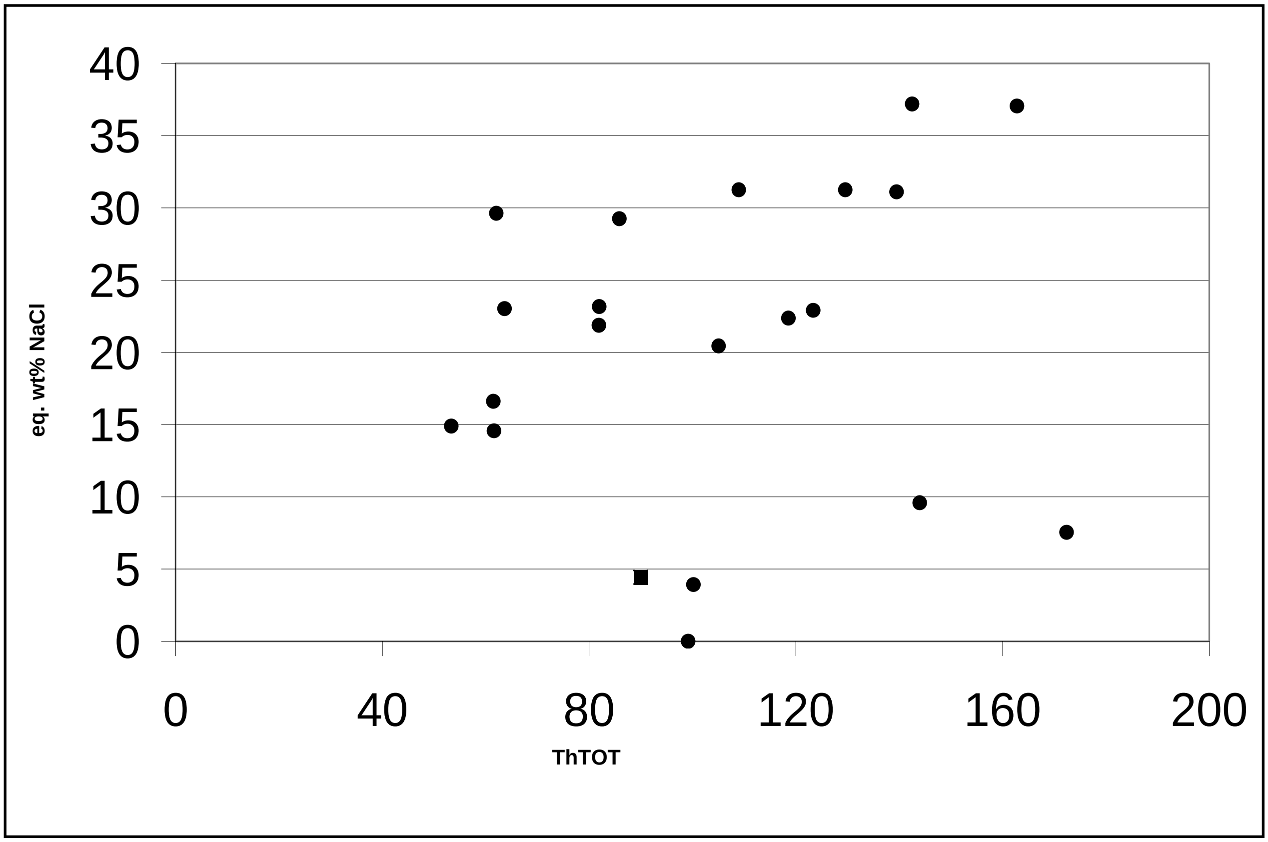


**Fig. 12B.** Equivalent wt% NaCl versus total homogenization temperature (ThTOT) for fluid inclusions from stages 1, 2 and 3.

**Table 2 -** LA-ICPMS analysis results of selected fluid inclusions in four samples. Values are in ppm, point means the position/fluid inclusion that underwent analysis, negative values = below detection limit.

| Point | Na23 | Mg24 | K39 | Ca43 | Cr53 | Mn55 | Fe56 | Fe57 | Ni60 | Cu65 | Zn66 | Zn67 | As75 | Rb85 | Sr88 | Ag107 | Sb121 | Cs133 | Ba138 | Au197 | Pb208 | Bi209 |
|---|---|---|---|---|---|---|---|---|---|---|---|---|---|---|---|---|---|---|---|---|---|---|
| **LD7113A/42.80m** | | | | | | | | | | | | | | | | | | | | | | |
| **A-18a** | 19670 | 181 | 6049 | 5057 | -56 | 139 | -489 | 1025 | 62 | -11 | 64 | 99 | 607 | 8 | 14 | 5 | 2 | 2 | 48 | -3 | 26 | -1 |
| **A-18b** | 19670 | 1555 | 4911 | 187180 | -140 | 3808 | 2730 | 3273 | -24 | 76 | 232 | 337 | 764 | 11 | 67 | -2 | 36 | 4 | 1444 | -6 | 149 | -3 |
| **A-18c** | 19670 | 1909 | 5179 | 267866 | -125 | 4966 | 5890 | 3638 | -22 | 96 | 261 | 442 | 827 | 10 | 94 | -2 | 37 | 4 | 1949 | -6 | 190 | -2 |
| **LD7113A/67.50m** | | | | | | | | | | | | | | | | | | | | | | |
| **A-4** | 48000 | 64 | 7673 | -53190 | -605 | 658 | -6282 | -2117 | 89 | 923 | 228 | 529 | 3317 | -14 | 280 | -10 | 140 | -12 | 58 | -23 | 960 | -10 |
| **A-1** | 48000 | 1011 | 7106 | 25086 | -147 | 741 | 10037 | 5262 | 139 | 645 | 855 | 3050 | 1328 | 29 | 279 | 19 | 116 | 7 | 90 | -4 | 783 | 10 |
| **A-8** | 48000 | 7827 | 5907 | 9591 | 29 | 69 | 1515 | 754 | 107 | 26 | 61 | 44 | 481 | 15 | 44 | 0 | 11 | 3 | 61 | -1 | 280 | 0 |
| **A-6** | 48000 | 4078 | 8068 | 4132 | -24 | 33 | 10258 | 3847 | 105 | 142 | 53 | 47 | 309 | 22 | 127 | 1 | 18 | 5 | 39 | -1 | 22 | 1 |
| **F-2 (2a)** | 33440 | 1967 | 6932 | 24506 | 117 | 390 | 10567574 | 1846222 | 1232 | 1108 | 359 | 351 | 2557 | 30 | 299 | 7 | 209 | 21 | 60 | -4 | 694 | 112 |
| **F-2 (3a)** | 33440 | 467 | 9994 | -6662 | 189 | 179 | 315689 | 108757 | 70 | 31 | 137 | 193 | 14838 | 35 | 278 | -3 | 34 | 12 | 97 | -4 | 997 | 3 |
| **A-2a** | 33440 | 40 | 4745 | -8525 | -124 | 152 | -4713 | 776 | -35 | 339 | 140 | 112 | 823 | 19 | 234 | -2 | 64 | 5 | 16 | -6 | 385 | -3 |
| **A-2b** | 33440 | 4805 | 3952 | 18875 | 1401 | 390 | 42320 | 8139 | 21191 | 408 | 707 | 311 | 3880 | 12 | 318 | 6 | 47 | -3 | 184 | -6 | 506 | -5 |
| **F-2 (2b)** | 33440 | 464 | 7439 | 43057 | -57 | 499 | 2639469 | 438221 | 280 | 88 | 138 | 87 | 914 | 16 | 453 | -1 | 42 | 7 | 27 | -3 | 96 | 2 |
| **F-2 (3b)** | 33440 | 155 | 9533 | -3577 | -59 | 73 | 41794 | 468 | 15 | 14 | 23 | 34 | 2090 | 18 | 228 | -2 | 39 | 7 | 34 | -2 | 446 | -1 |
| **F-2 (3c)** | 33440 | 32 | 7771 | -5257 | -86 | 129 | -2790 | -450 | -19 | -14 | -16 | -39 | 2070 | 17 | 197 | -2 | 98 | 6 | 4 | -3 | 1220 | -2 |
| **LD7113A/135.50m** | | | | | | | | | | | | | | | | | | | | | | |
| **B-13a** | 26790 | 1715 | 24613 | 15946 | 252 | 217 | 7850 | 3872 | 784 | 28 | 207 | 244 | 353 | 30 | 292 | -1 | 48 | 6 | 1587 | -3 | 563 | -1 |
| **B-13b** | 26790 | 44023 | 390370 | -269847 | -4226 | -660 | 86370 | 87351 | -687 | -1009 | -1105 | -3857 | -1452 | 497 | 1203 | -68 | -131 | -58 | 45174 | -134 | 807 | -69 |
| **B-104** | 26790 | 2486 | 25645 | -17582 | 251 | 474 | 36372 | 11618 | 137 | 429 | 1126 | 1250 | 230 | 51 | 269 | 6 | 69 | 5 | 1098 | -13 | 731 | -5 |
| **E-206** | 42330 | 54 | -260 | 6848 | -121 | -15 | -1979 | -459 | -24 | -18 | -25 | 77 | -36 | -2 | 495 | -2 | -3 | -1 | 182 | -4 | 8 | -2 |
| **E-207** | 42330 | 152 | 105 | 452 | -3 | 1 | -30 | 21 | -1 | 2 | 1 | -2 | 2 | 0 | 7 | 0 | 0 | 0 | 2 | 0 | 1 | 0 |
| **E-208** | 42330 | 5187 | 2301 | 9688 | 118 | 299 | 18601 | 12410 | 1172 | 132 | 325 | 299 | 25 | 8 | 255 | -1 | -1 | 1 | 98 | -1 | 15 | 18 |
| **B-104** | 26790 | 5369 | 19461 | -77327 | -1083 | 270 | -18072 | 10906 | -327 | -225 | 732 | -911 | -488 | 64 | 462 | -24 | 127 | 15 | 1097 | -59 | 1965 | -22 |
| **LD7113A/173.05m** | | | | | | | | | | | | | | | | | | | | | | |
| **B-21** | 15066 | 7118 | 7710 | -18527 | 280 | 78 | 2353 | 3278 | 255 | 2075 | 384 | 1849 | 107 | 11 | 106 | -4 | 23 | -4 | 108 | -9 | 105 | -4 |
| **B-209** | 15066 | 9987 | 16270 | 20322 | -253 | 43 | 20513 | 8255 | 106 | 4761 | 312 | 338 | 372 | 42 | 195 | 7 | 51 | -3 | 1493 | -7 | 233 | 350 |
| **B-210** | 15066 | 3080 | 22280 | 7682 | -144 | -21 | 10764 | 10494 | 278 | 1330 | 123 | 310 | 116 | 35 | 233 | -2 | 11 | 3 | 2093 | -6 | 216 | -2 |

**Table 3 -** PIXE analysis results of selected fluid inclusions in two samples. Values are in ppm, Point means the position/fluid inclusion that underwent analysis.

| point | Cl | K | Ca | Ti | Mn | Fe | Cu | Zn | Ge | As | Br | Rb | Sr | Mo | Ru | Ag | Sn | Sb | Cs L | Ba L | Pb L |
|---|---|---|---|---|---|---|---|---|---|---|---|---|---|---|---|---|---|---|---|---|---|
| **LD7113A/67.50m** | | | | | | | | | | | | | | | | | | | | | |
| **A-9** | deep | 48035 | 145817 | <1321 | 841 | 19499 | 848 | <626 | <650 | 890 | 1115 | <1310 | <1388 | <2997 | <4811 | <8839 | <16833 | <21977 | 10087 | 12371 | 2004 |
| **A-12** | 39768 | 6875 | 32747 | <484 | 753 | 10376 | <471 | 880 | 799 | <304 | 645 | <1072 | <1060 | <2282 | <3639 | <6615 | <12468 | <15347 | 3942 | 3145 | 1138 |
| **F-1** | deep | 191121 | 467157 | <533 | 3415 | 10983 | <251 | 637 | 202 | <160 | 1902 | <696 | 26431 | 771 | <960 | <1762 | <3353 | <4377 | <2705 | 12474 | 3683 |
| **F-2** | deep | 7771 | 5752 | <183 | <97 | 5209 | 94 | <69 | 117 | 124 | <104 | <183 | <197 | <430 | <689 | <1260 | <2389 | <3115 | 1742 | 1257 | <113 |
| **F-4** | deep | 14056 | 15630 | <245 | 215 | 9411 | 688 | 123 | <62 | 1386 | 253 | <171 | 385 | <387 | <621 | <1142 | <2176 | <2687 | 2627 | 3850 | 462 |
| **F-6** | 8025 | 3130 | 2042 | <93 | <71 | 5512 | 305 | 102 | <48 | 274 | 158 | <115 | 158 | <248 | <397 | <723 | <1365 | <1681 | 551 | 582 | 103 |
| **F-7** | 17099 | 1834 | 612 | <58 | <35 | 803 | 64 | 31 | <38 | 106 | <100 | <159 | <189 | <421 | <673 | <1229 | <2460 | <3033 | 322 | 308 | <109 |
| **F-8** | 29407 | 11031 | 16323 | <240 | 349 | 7010 | 200 | 238 | <79 | 1079 | 271 | <233 | 374 | <528 | <847 | <1551 | <2945 | <3634 | 2014 | 1177 | 983 |
| **F-102** | 23286 | 6988 | 8066 | <743 | <575 | 16373 | 1045 | 970 | <569 | 985 | <1505 | <2388 | <2855 | <6295 | <10039 | <18255 | <34412 | <44786 | 5744 | 3144 | <1654 |
| **LD7113A/ 135.50m** | | | | | | | | | | | | | | | | | | | | | |
| **B2-13** | deep | 2851 | 8001 | <244 | <126 | 234 | <122 | <117 | 135 | <99 | 229 | <268 | 2267 | <669 | <1008 | <1951 | <3703 | <4569 | 1382 | 1834 | 411 |
| **E-14** | 282367 | 383168 | 13643 | 1832 | <586 | 89555 | 685 | <528 | 964 | 889 | <607 | <1737 | <1270 | <2694 | <4309 | <7869 | <14897 | <18362 | 8574 | 21335 | <773 |
| **E2-15** | 373583 | 102869 | 35334 | <1024 | <666 | 51424 | 745 | 5403 | 676 | <753 | 4266 | <3250 | 9842 | <6436 | <10259 | <18644 | <35128 | <43235 | <4626 | 12398 | 6707 |
| **E-16** | 34542 | 38404 | 8567 | <558 | <272 | 33699 | 317 | 431 | 431 | 658 | <329 | <598 | <680 | <1476 | <2220 | <4324 | <8197 | <10109 | 5700 | 10223 | <389 |
| **E-107** | <12242 | 142575 | 34365 | 1818 | <773 | 78287 | 1026 | <764 | 660 | 858 | <1231 | <2548 | <2566 | <5521 | <8813 | <16047 | <30290 | <37305 | 8756 | 13627 | <1432 |
| **B-21** | 16358 | 5341 | 6772 | <426 | <330 | 19102 | 3104 | 333 | <279 | 511 | <742 | <1224 | <1407 | <3085 | <4913 | <8917 | <16777 | <21819 | <1861 | 3866 | <837 |
| **B-22** | 74921 | 4792 | 5934 | <708 | <502 | 15160 | 1147 | 905 | 775 | 571 | <1113 | <1760 | <2121 | <4652 | <7423 | <13488 | <25420 | <33080 | 5298 | 4993 | <1203 |
| **B2-2** | 70340 | 6258 | 11880 | <636 | <414 | 36172 | 1038 | 456 | 638 | <395 | <785 | <1378 | 1622 | <3436 | <5478 | <9957 | <18763 | <23096 | 7281 | 4358 | <958 |
| **B-23** | 265547 | 19266 | 57069 | <1516 | <877 | 57665 | 986 | 1102 | 1220 | <636 | 1989 | <2332 | 7837 | <5474 | <8736 | <15910 | <30036 | <36994 | 14700 | 19642 | 3511 |

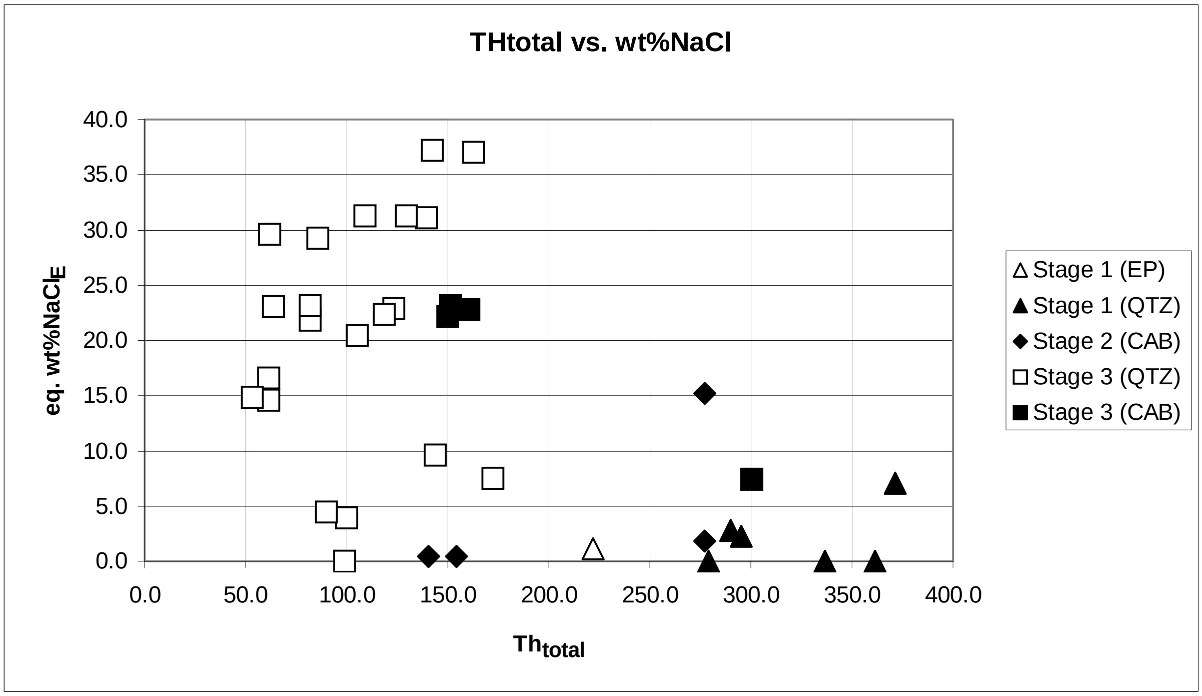


**Fig. 13A.** Equivalent weight % NaCl versus total homogenization temperature.

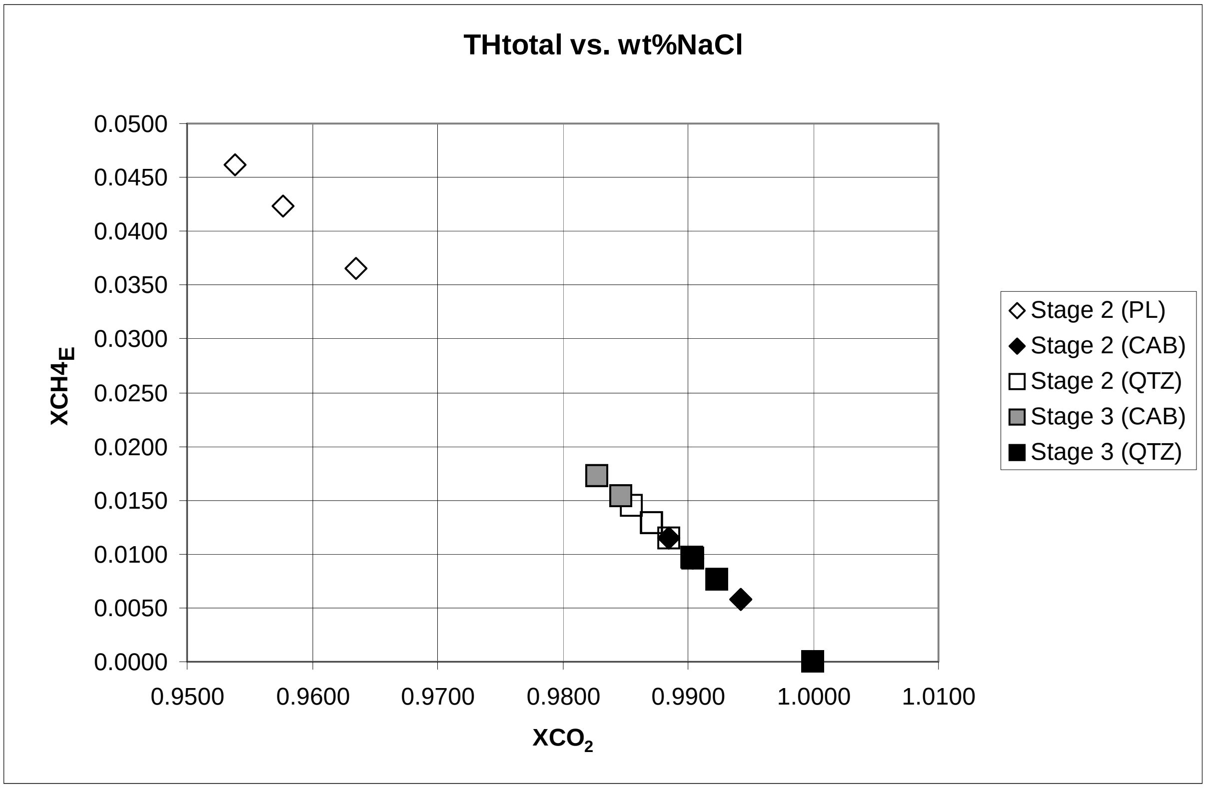


**Fig.13B.** $XCH_4$ versus $XCO_2$.

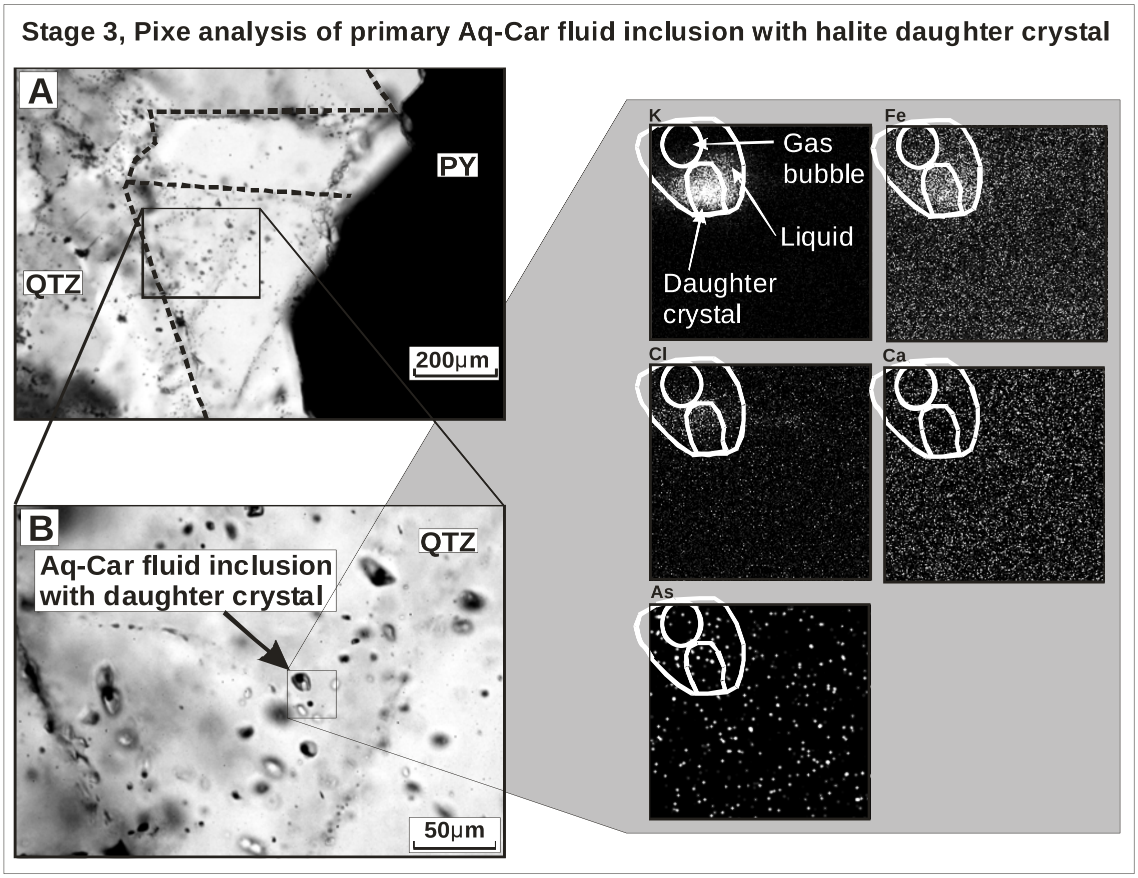


**Fig. 14A.** Euhedral quartz crystal has grown from a pyrite crystal (post-pyrite); **B.** Primary Aq-Car fluid inclusion with a halite daughter crystal that was analysed with PIXE; **C.** PIXE image for K, Fe, Cl, Ca and As. Important to note that these late fluid inclusions (stage 3) trapped only halite as daughter crystal, no calcium was detected in the inclusion like from stage 2.

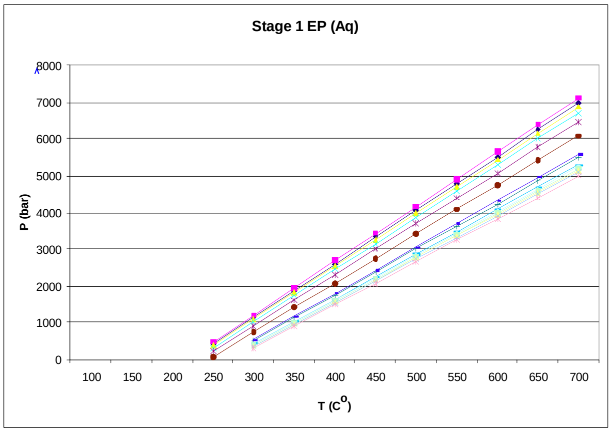


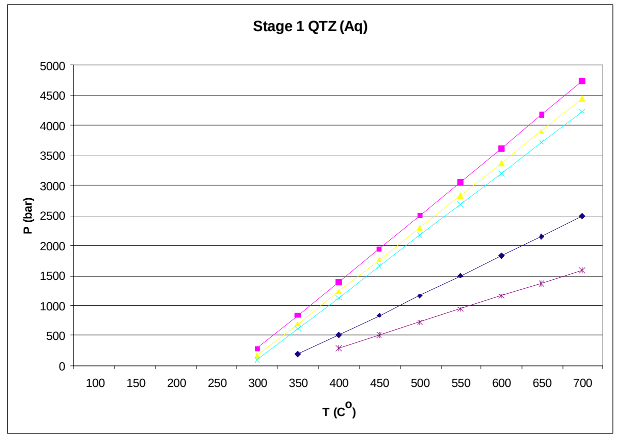


**Fig. 15A.** Selected isochores for aqueous inclusion associated with stage 1 hydrothermal alteration.

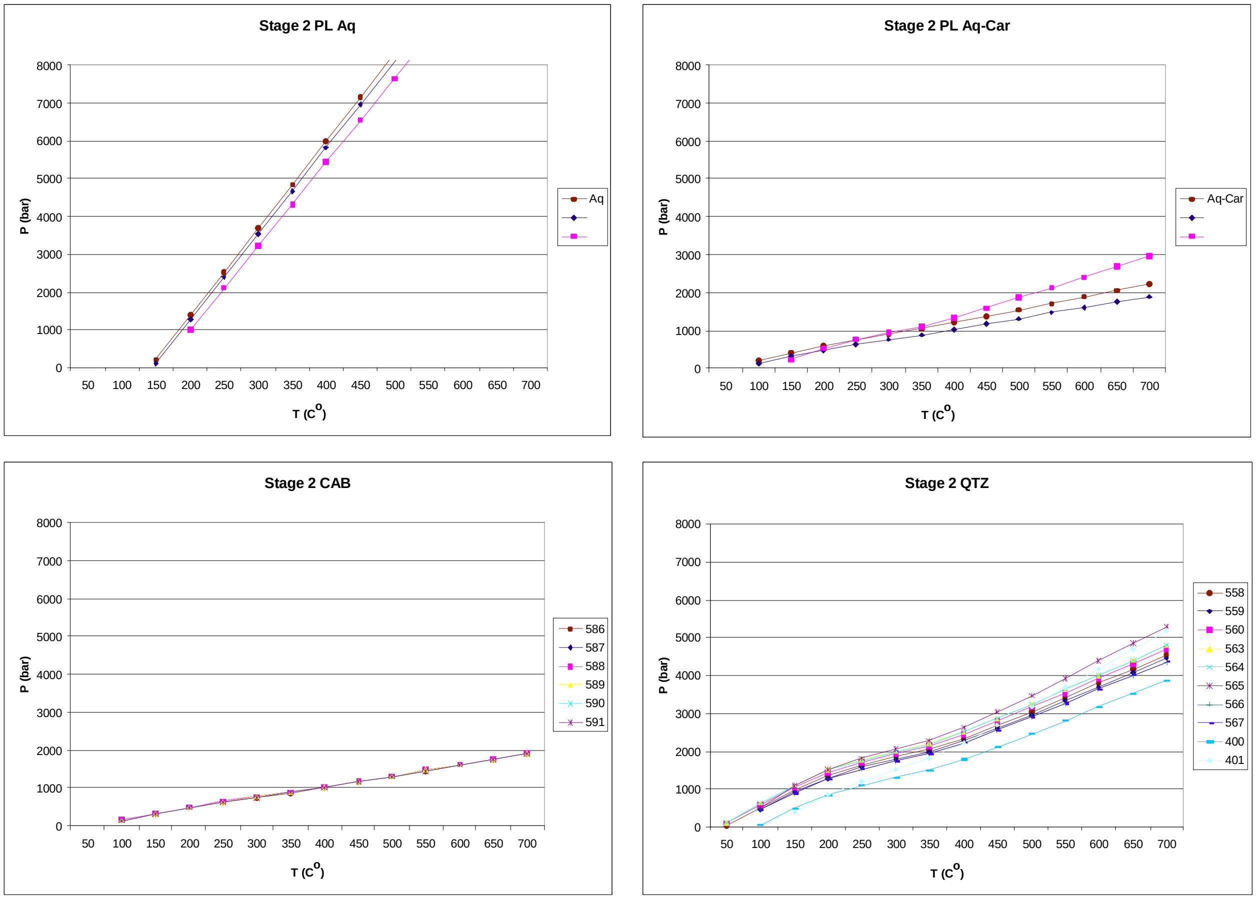


**Fig. 15B.** Selected isochores for aqueous and aqueous-carbonic inclusion associated with stage 2 hydrothermal alteration.

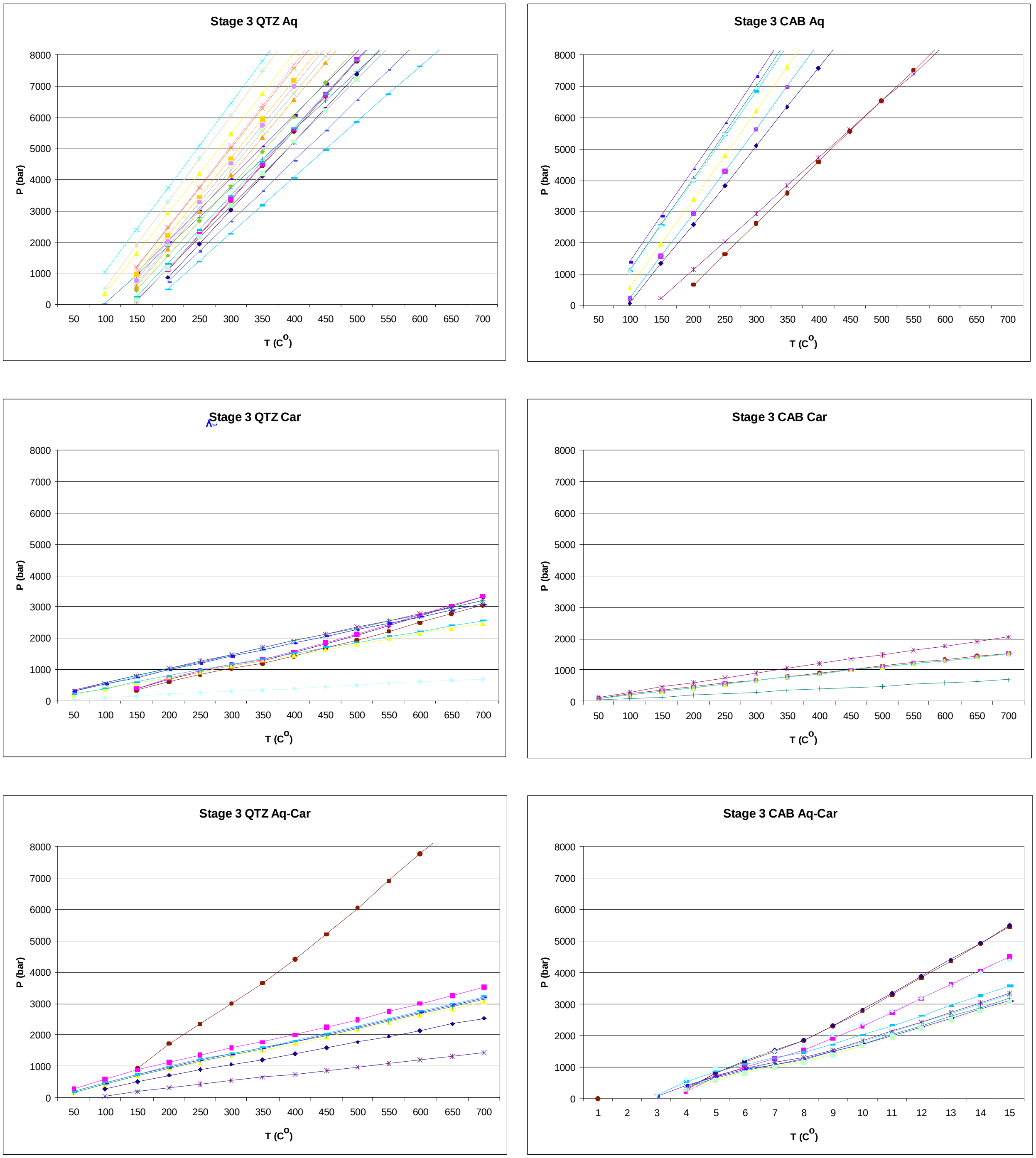


**Fig. 15C.** Selected isochores for aqueous, aqueous-carbonic and carbonic inclusion associated with stage 3 hydrothermal alteration.